Quantitative spatial profiling of NSCLC subtypes across tumor stages using 6-plex multiplex imaging technology and AI-powered phenotyping analysis

Lorcan Sherry[1], Bethany Remeniuk[2], Karen McClymont[1], Bei Hopkins[2], Natalie Monteiro[2], Nicole Couper[1], Gabriel Reines March[1], Darren Locke[2]

[1]OracleBio Ltd, Glasgow, Scotland, UK [2]Akoya Biosciences, Inc, Marlborough, Massachusetts, USA

OracleBio AKOYA BIOSCIENCES **Email Contacts**: lorcan.sherry@oraclebio.com | dlocke@akoyabio.com | bremeniuk@akoyabio.com

Background

Non-small cell lung cancer (NSCLC) is a complex disease with varying pathological subtypes including adenocarcinomas (ADC) and squamous cell carcinomas (SSC). After diagnosis, pathological Tumor-Node-Metastasis (pTNM) staging provides important information about the extent of cancer in the body and anticipated response to treatment. NSCLC patients can have impaired immune responses within the tumor microenvironment (TME), leading to a progression of tumor growth and poorer prognosis. Accurate cell phenotyping combined with spatial profiling of the immune contexture and checkpoint expression, can provide a deeper understanding of complex cellular interactions underpinning the tumor-immune response.

The aim of this study was to utilize spatial multiplexed imaging technology and associated data analysis methods to profile the immune contexture, as well as their spatial interactions with the tumor, in a set of tissue cores covering a range of NSCLC subtypes and tumor staging.

Methods

Formalin-fixed paraffin-embedded (FFPE) NSCLC tissue microarrays (TMA), comprised of n=38 cores (Figure 1) containing a range of carcinomas and pTNM stages (I-IV), were stained on a Leica Bond RX™ using the Akoya PhenoCode™ Signature Immuno-contexture Human Protein Panel, which includes markers for CD8, CD68, PD-1, PD-L1, FoxP3, and PanCK as a tumor indicator. Stained TMAs were scanned at 20x magnification on a PhenoImager® HT multispectral imaging system.

N=36 cores passed image QC and progressed to image analysis using Visiopharm software. Deep Learning algorithms were developed to segment each core into tumor and stroma regions of interest (ROI) and to accurately detect and classify different cell populations. A DeepLabv3+ neural network was used to develop the classifier using DAPI and PanCK input channels (Figure 2). A customized cell analysis algorithm was trained using a U-Net neural network to detect individual cell lineages and subsequent phenotypes of interest (Figures 3 & 4). A specific deep learning approach was initially taken to form CD8, CD68 and DAPI cell objects by generating training labels for the 3 cell types across the TMA cores and using the 3 markers as input channels for Deep Learning training. A hierarchical post processing approach was then applied to create CD8, CD68, PanCK and remaining DAPI cell objects for downstream phenotyping.

Cell object data per core was generated from Visiopharm software and spatial analysis performed using an OracleBio proprietary program (PhenoXplore) to calculate readouts for neighborhood analysis for selected phenotypes.

Results

Immune cell counts, phenotypes and spatial interactions were identified within the tumor and stroma ROI *per* core. Data included total and negative cell phenotype counts, cell density in tumor and stroma, as well as neighboring spatial interactions in each of the 36 cores in the TMA set.

ADC and SSC cores showed variable amounts of immune inflammatory phenotypes within tumor and stroma ROI (Figure 5A). In ADC cores, dual CD8+ PD-1+, single FoxP3 + and single PD-1+ cells (possibly CD4+) showed the highest mean counts, while in SCC cores CD8+ PD-1+, single PD-1+ and single CD68+ cells showed the highest mean counts. All cores contained tumor and stroma ROI to varying levels (Figure 5B.)

CD8/FoxP3 immune cell ratios across pTNM grades demonstrated varying ranges, with some cores showing high CD8/FoxP3 ratio and other cores showing high FoxP3/CD8 ratios. No general relationship was observed for ratios across increasing pTNM grades (Figure 5C).

Cell spatial relationships across cores is shown in Figure 6. A trend was observed for a higher % of immune cells and higher % of macrophages within 20µm of a tumor cell in cores from pTNM combined grades I & II compared to combined grades III & IV.

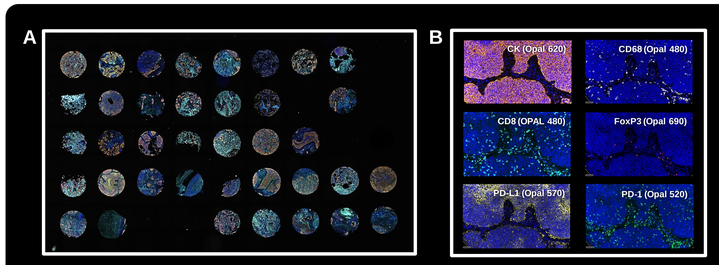

Figure 1: A. NSCLC TMA overview (n=38 cores); B. example staining *per* marker channel.

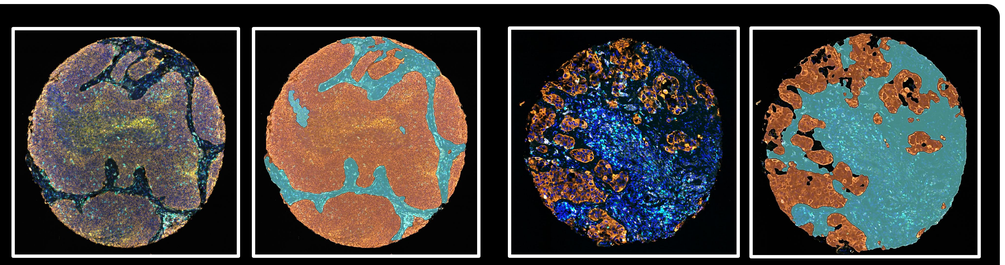

Figure 2: Example deep learning classification of tumor (orange overlay) and stroma (cyan overlay) ROI across 2 cores.

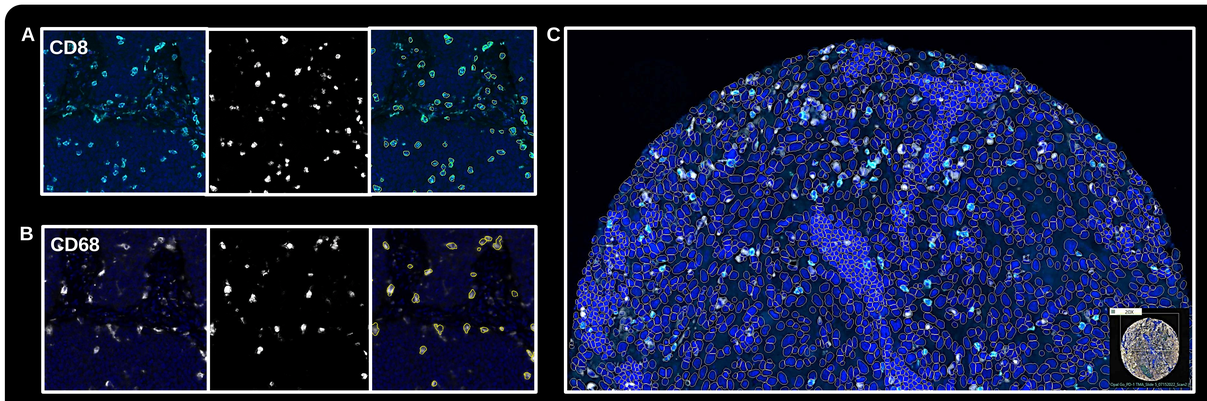

Figure 3: (A and B) Example cell analysis detection using deep learning showing fluorescent channel only, probability map generation and cell formation for CD8 and CD68 marker channels; **(C)** overview of deep learning cell formation across whole core using CD8 (cyan), CD68 (white) and DAPI (blue) input channels.

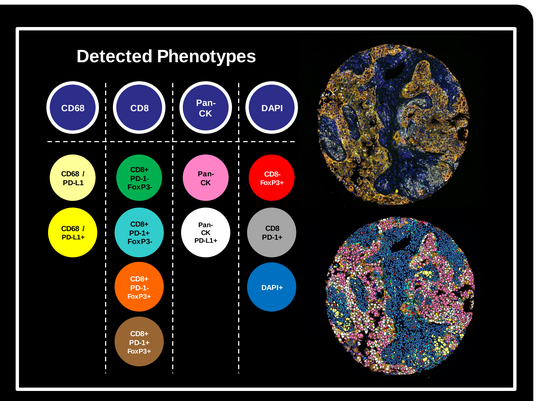

Figure 4. List of detected phenotypes with example whole core cell classification overlay.

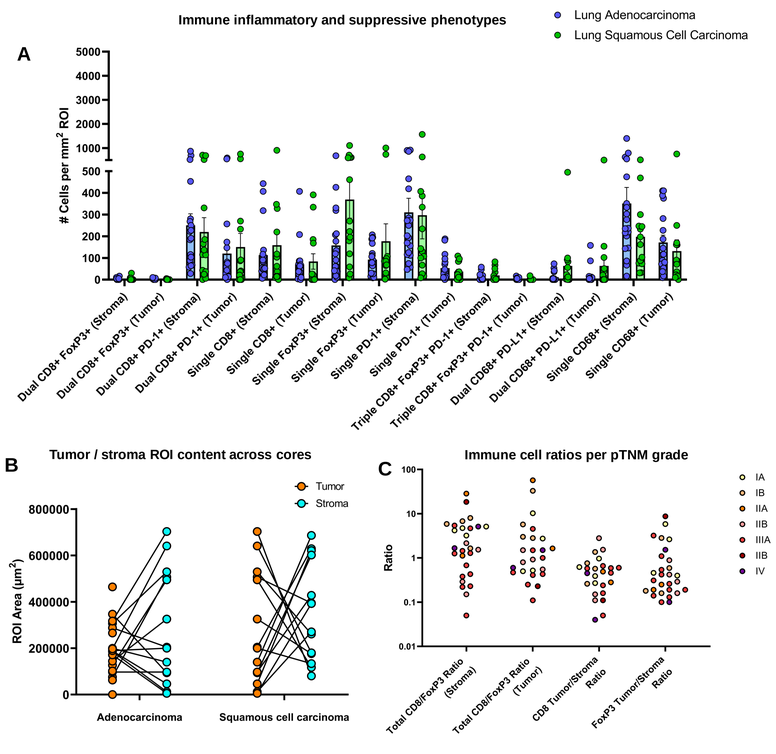

Figure 5: Graphs showing (A) Immune inflammatory and suppressive phenotypes within tumor and stroma ROI across ADC and SSC cores; (B) Tumor Stroma ROI content per core; and (C) Immune cell ratios per core across different pTNM grades.

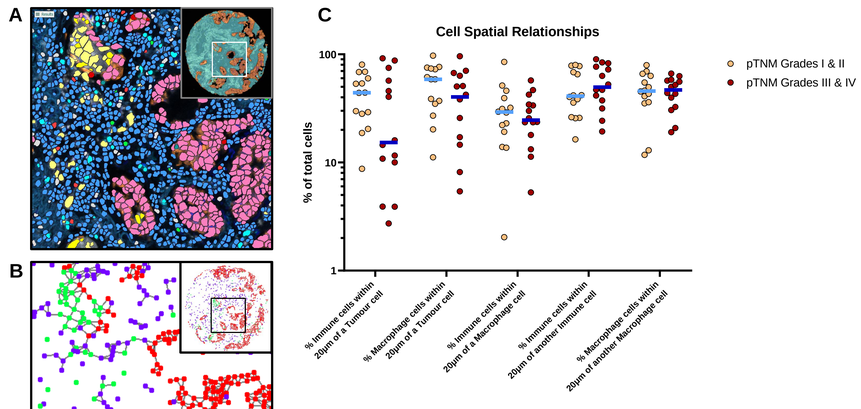

Figure 6: (A) Example cell phenotype analysis and **(B)** spatial overlay showing vector locations of CD8 (purple), CD68 (green) and Pan CK (red) phenotypes within the TME of a core; **(C)** graph of cell spatial relationships across cores grouped based on pTNM grades 'I & II' or 'III & IV'. Immune cells category in figure exclude macrophages.

Conclusions

The combination of high quality, spatial phenotyping data provided by the PhenoCode Signature Panel, coupled with Deep Learning quantitative image analysis techniques, enables detailed characterization of cell phenotypes and spatial arrangements across tumor subtypes and pTNM grades of NSCLC tissue. This study further highlights the importance of a robust technical workflow to deliver optimal staining, imaging, cell detection and phenotyping paving the way to generate high quality data that can provide a deeper understanding of complex immune-tumor interactions. Such data can further support evaluation of therapeutic target validation, target prevalence and biomarker interactions to help drive informed R&D decision making.